

A unique small-scale gravitational arc in Abell 1201¹

Alastair C. Edge,² Graham P. Smith,³ David J. Sand,³ Tommaso Treu,^{3,4,5} Harald Ebeling,⁶
Steven W. Allen,⁷ Pieter G. van Dokkum,^{3,8}

ABSTRACT

We present a snapshot *Hubble Space Telescope (HST)* image of the galaxy cluster A 1201 ($z=0.169$), revealing a tangential arc 2 arcsec from the brightest cluster galaxy (BCG). Keck–ESI spectroscopy confirms that the arc is gravitational in nature and that the source galaxy lies at $z=0.451$. We construct a model of the gravitational potential of the cluster that faithfully reproduces the observed arc morphology. Despite the relaxed appearance of the cluster in the *HST* frame, the best fit ellipticity of the total matter distribution is $\epsilon_{\text{total}} \geq 0.5$, in contrast to the light distribution of the BCG ($\epsilon_{\text{BCG}} = 0.23 \pm 0.03$) on 2'' scales. Further deep optical observations and pointed X-ray spectro-imaging observations with *Chandra* are required to determine whether this elongation is due to a single elongated dark matter halo, or a more complex distribution of matter in the cluster core. We compare the arc with a sample drawn from the published literature, and confirm that it is unique among tangential systems in the small physical scales that it probes (~ 6 kpc). In anticipation of a more thorough investigation of this cluster across a broad range of physical scales, we use our fiducial lens model to

¹Based on observations at the Keck Observatory, which is operated jointly by the California Institute of Technology and the University of California, and with the NASA/ESA Hubble Space Telescope, obtained at Space Telescope Science Institute, which is operated by the Association of Universities for Research in Astronomy, under NASA contract NAS5-26555.

²Department of Physics, University of Durham, South Road, Durham DH1 3LE, UK

³California Institute of Technology, Department of Astronomy, Mail Code 105–24, Pasadena, CA91125, USA

⁴Department of Physics and Astronomy, University of California at Los Angeles, Los Angeles, CA 90095, USA

⁵Hubble Fellow

⁶Institute for Astronomy, 2680 Woodlawn Drive, Honolulu, HI 96822, USA

⁷Institute of Astronomy, University of Cambridge, Madingley Road, Cambridge CB3 0HA, UK

⁸Department of Astronomy, Yale University, New Haven, CT 06520, USA

estimate the projected mass and mass-to-light ratio of the cluster within a radius of 6 kpc, obtaining: $M=(5.9^{+0.9}_{-0.7})\times 10^{11} M_{\odot}$, $M/L_V=9.4^{+2.4}_{-2.1}(M/L)_{\odot}$. Overall our results confirm the importance of *HST* snapshot surveys for identifying rare lensing constraints on cluster mass distributions. In combination with follow-up optical and X-ray observations, the arc in A 1201 should help to increase our understanding of the physics of cluster cores.

Subject headings: galaxies: gravitational lensing — galaxies: clusters — galaxies: individual: A 1201

1. Introduction

Galaxy clusters are important laboratories in which to study physical processes that are generally inaccessible in other environments. For example the radial density profile and the projected ellipticity of clusters on the sky may offer valuable clues into the nature of dark matter (e.g., Spergel & Steinhardt 2001; Sand et al. 2002; 2003; Miralda-Escudé 2002; Arabadjis et al. 2002). Complications often arise in cluster-based studies of dark matter due to the presence of baryons (e.g., Allen 1998; Smith et al. 2001; Lewis et al. 2003). However, from a broader perspective such complications provide us with important clues into the physics of gas cooling, and inter-play between baryons and dark matter, both of which are central to attempts to understand the physics of galaxy formation (e.g., Cole et al. 2000).

Progress towards these goals requires detailed study of the distribution of mass in clusters. Strong gravitational lensing offers a direct and precise probe of cluster mass distributions (e.g., Kneib et al. 1996; Smith 2002; Smith et al. 2003). Complementary constraints can also be obtained from X-ray observations (e.g., Allen et al. 2002), weak lensing (e.g., Kneib et al. 2003) and the three-dimensional distribution of cluster galaxies (e.g., Czoske et al. 2002). A combination of these techniques is necessary for a comprehensive understanding of mass in clusters. Armed with the results from such multi-wavelength studies, robust constraints on the dark matter particle and gas cooling may ultimately flow.

We have conducted a snapshot survey of 55 X-ray luminous galaxy clusters with the WFPC2 camera on-board *HST* (PID's 8301 & 8719; PI Edge). A key goal of this survey is to uncover new cluster lenses with which to explore the questions outlined above. The snapshot observing strategy is well-suited to identifying clusters containing rare and powerful constraints such as radial arcs (e.g., RXJ 1133 – Sand et al. 2003).

In this letter we present an *HST* observation of A 1201 ($z=0.169$; $(\alpha, \delta)=11^h13^m01.1^s+13^{\circ}25'40''$ [J2000]; $L_X=(3.7\pm0.8)\times 10^{44}$ erg/s [0.1–2.4 keV] – Ebeling et al. 1998). These data reveal a tangential

arc 2" from the optical centroid of the BCG. Spectroscopic observations at the Keck Observatory confirm that the arc is a gravitationally-lensed galaxy at $z=0.451$ (§2). The best-fit gravitational lens model faithfully reproduces the arc morphology, however the total matter distribution of this model appears to be much more elongated than the optical isophotes of the BCG (§3). We also discuss the uniqueness of this small-scale gravitational arc by comparing it with other known cluster lenses, and outline how follow-up optical and X-ray observations will help to fully exploit this powerful new constraint on the matter distribution in cluster cores (§4). We assume $H_0=65 \text{ km s}^{-1}\text{Mpc}^{-1}$, $\Omega_M=0.3$ and $\Omega_\Lambda=0.7$. In this cosmology, $1''\equiv 3.1 \text{kpc}$ at $z=0.169$ and $1''\equiv 6.2 \text{kpc}$ at $z=0.451$.

2. Observational Data and Analysis

2.1. *Hubble Space Telescope Imaging*

A 1201 was observed through the F606W filter with *HST* using the WFPC2 camera on April 7, 2001. We combined the 2×400 -sec exposures into a single mosaic using standard IRAF tasks, and present in Fig. 1 the region of the WF3 chip ($5''\times 5''$) that contains the central galaxy. This frame reveals a tangentially distorted arc at a radius of 2" from the optical centroid of the BCG. We interpret this arc as arising from the gravitational distortion of a background galaxy by the foreground cluster potential.

2.2. Keck-ESI Spectroscopy

The arc was observed with the Echelle Imaging Spectrograph (ESI – Sheinis et al. 2002) on the Keck-II 10-m telescope on the night of April 12, 2002, in $0.6''$ seeing. These observations and the reduction of the data are described in detail by Sand et al. (2003). In summary, a $1.25''\times 20''$ slit was centered on the BCG, oriented to intersect the portions of the arc labeled A1b and A1c in Fig. 1. The total integration time was 7.2-ksec. The final reduced spectrum covers the wavelength range $5300 \leq \lambda_{\text{obs}} \leq 9800 \text{\AA}$, and contains [OII (3726,3729)], H β , [OIII (4959,5007)] and H α at $\lambda_{\text{obs}}=(5406.7, 5410.8)$, 7053.5, (7195.3,7264.7), 9523.1 \AA respectively, in addition to numerous other emission and absorption features. From these spectral features, we derive a redshift of $z=0.451$ for the arc, thus confirming the gravitational lensing interpretation.

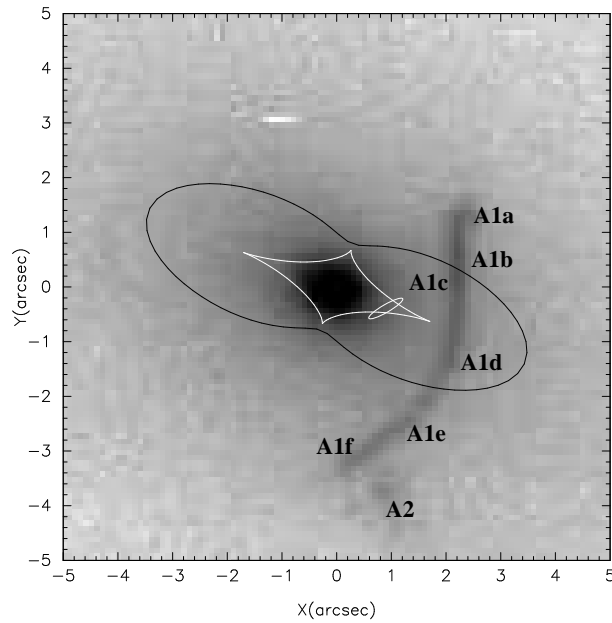


Fig. 1.— Zoom into the central $5'' \times 5''$ of the WF3 chip, showing the detailed morphology of the arc and the multiple-image identification upon which our lens model is based (§3). The solid black curve shows the $z=0.451$ tangential critical curve and the white astroid shows the $z=0.451$ caustic curve in the source plane. The white ellipse shows a schematic view of the orientation and position of the galaxy in the source plane and reveals how it lies across the caustic, giving rise to the distinctive observed arc morphology.

2.3. Multiple-image Interpretation

We label the different segments of the arc (A1) in Fig. 1, together with the faint feature that lies within $1''$ of the lower end of the arc (A2). The relatively high surface brightness of A1b/c and the dip in surface brightness between this pair implies that they are a pair of fold images arising from a portion of the galaxy that straddles the $z=0.451$ caustic in the source-plane. The de-magnified counter-image of this pair would then most likely be A1f. The position angle break between A1d and A1e probably arises from a combination of the source-plane morphology of the lensed galaxy and its orientation relative to the caustic curve. The emission from these two regions has insufficient signal-to-noise to support definitive statements regarding the multiple-image interpretation of A1d/e and indeed A1a. However given their similarities in surface-brightness, it is plausible that A1a/d/e are three images of the same portion of the galaxy.

3. Gravitational Lens Modeling

3.1. A simple “relaxed” model

We construct a model of the projected mass distribution in A1201 using the LENSTOOL software developed by Kneib (1993; see also Kneib et al. 1996). The model consists of a single lens plane at $z=0.169$, comprising two mass components (cluster-scale dark matter halo and BCG) that we parametrize as truncated pseudo-isothermal elliptical mass distributions (PIEMD – Kassiola & Kovner 1993). The projected cluster mass distribution is therefore described by fourteen parameters: $x_c, y_c, \epsilon, \theta, r_{\text{core}}, r_{\text{cut}}, \sigma_0$ for each of the two mass components. We match the central coordinates (x_c, y_c) for each component to the optical centroid of the BCG, as measured from the *HST* frame. We also match the ellipticity ($\epsilon=0.23\pm0.03$) and position angle ($\theta=-(21\pm1)^\circ$) of these two mass components to that of the observed light distribution measured at $R=2''$. Typical values of r_{core} and r_{cut} for cluster-scale mass components are 50–100kpc and \gtrsim 500kpc respectively (Smith 2002) – i.e. well beyond the physical scales probed by the arc in this cluster. We therefore fix these two parameters at 75kpc and 1000kpc respectively – we find that none of the results described below are sensitive to these choices. This leaves just four free parameters: the central velocity dispersion (σ_0) of the cluster and the core radius, cut-off radius and central velocity dispersion ($r_{\text{core}}, r_{\text{cut}}, \sigma_0$) of the BCG.

We first constrain these parameters using the image pair A1b/c and the location of the $z=0.451$ critical line that bisects these images. This model is an acceptable fit to these constraints ($\chi^2/\text{dof}\simeq 1$ – see Smith 2002 for a detailed explanation of how goodness-of-fit

is estimated for such lens models), however it predicts that the counter-image of A1b/c lies $\sim 0.5''$ closer to the center of the lens than the observed location of the candidate counter images (i.e. A1e and A1f). When A1f is added to the model constraints, the fit deteriorates significantly ($\chi^2/\text{dof} \approx 100$). The most straight-forward way to improve the quality of this fit is to make the mass distribution more elliptical. We therefore include the ellipticity of the cluster-scale dark matter halo as a free parameter in the fit. This yields an acceptable fit for values of $\epsilon_{\text{DM}} \geq 0.7$. This lower limit on the cluster ellipticity is insensitive to whether A1e or A1f are adopted as the third counter image of A1b/c. We also experiment with holding the ellipticity of the dark matter fixed at $\epsilon_{\text{DM}} = 0.23$, and fitting for the ellipticity of the BCG, obtaining $\epsilon_{\text{BCG}} \geq 0.7$. Fixing $\epsilon_{\text{DM}} = \epsilon_{\text{BCG}}$ and fitting for the ellipticity of the total matter distribution, we obtain $\epsilon_{\text{DM}} = \epsilon_{\text{BCG}} \geq 0.5$. In summary, the underlying cluster total mass distribution appears to be significantly more elliptical than the spatial distribution of stars in the BCG.

3.2. Is A 1201 Bi-modal?

We also explore the possibility that A 1201 is bi-modal, and examine the *HST* data for evidence of a second cluster-scale mass clump. An $\sim L^*$ cluster galaxy lies on the WF2 chip in the same direction as the position angle of the cluster mass distribution, suggesting that a second mass clump may be associated with this galaxy. However, there are no other bright cluster members in this vicinity, indicating that this scenario is quite unlikely (Smith et al. 2002). Weak shear maps may also be used to infer the likely morphology of cluster mass distributions (e.g., Kneib et al. 1996), however the short exposure time of these *HST* data preclude such an analysis for A 1201 (we estimate that just ~ 100 suitable faint galaxies are available across the entire WFPC2 field of view). Despite the weak evidence for its existence, we quantify how massive a second cluster-scale dark matter halo would have to be in order to

Table 1: Fiducial Lens Model Parameters

Mass Component	x_c (arcsec)	y_c (arcsec)	$\epsilon^{(1)}$	$\theta^{(2)}$ (deg)	r_{core} (kpc)	r_{cut} (kpc)	σ_o (km/s)
Cluster	0.0	0.0	>0.7 ⁽³⁾	-21	75	1000	904
BCG	0.0	0.0	0.23	-21	0.7	150	197

¹ $\epsilon = (a^2 - b^2)/(a^2 + b^2)$ where a and b are the semi-major and semi-minor axes respectively.

² θ is measured anticlockwise from the positive X -axis in Fig. 1.

³ Quantities in bold are free parameters in the lens model.

explain the observed multiple–images. We fix the ellipticity of the central dark matter halo and BCG at $\epsilon=0.23$ and add a circular dark matter halo at the position of the bright cluster galaxy noted above. The best–fit velocity dispersion of this dark matter halo is $\sigma_o=1000\text{km/s}$ (with r_{cut} and r_{core} held fixed at 1Mpc and 50kpc respectively). In this bimodal model, the velocity dispersion of the central dark matter halo is $\sim 750\text{km/s}$, suggesting that if A 1201 is bimodal, then the dominant mass component would not be coincident with the BCG.

In summary, although a bi–modal mass distribution is allowed by the current shallow *HST* data, we suggest that an elliptical mass distribution is the more likely explanation of the strong lensing signal in this cluster. We also note that our forthcoming *Chandra* observations (PID: 04800980, PI: Edge) will be the first pointed X–ray observations of this cluster. The X–ray pass–band therefore currently offers no clues on the cluster mass distribution.

3.3. The Fiducial Model

We adopt the model described in §3.1 in which $\epsilon_{\text{BCG}}=0.23$ and $\epsilon_{\text{DM}}\geq 0.7$ as the fiducial lens model and list the relevant parameters in Table 1. We ray–trace each portion of the arc through the fiducial model back to the source–plane to double check our interpretation of the multiple–images. We summarize this exercise with the white ellipse in Fig. 1 which shows the position, size and orientation of the galaxy in the source–plane. A1 therefore appears to be an elongated galaxy, possibly an edge–on star–forming disk galaxy. The observed morphology of the arc may therefore be explained by a combination of the elongated source–plane morphology and the orientation of this galaxy relative to the caustic which we over–plot as the white astroid in Fig. 1. Integral field unit spectroscopic observations of this arc (e.g., Swinbank et al. 2003) would help to confirm our interpretation of the arc as arising from an edge–on galaxy.

We also use the fiducial model to measure the projected mass enclosed within the $z=0.451$ tangential critical curve, obtaining $M(R\leq 2'')=(5.9^{+0.9}_{-0.7})\times 10^{11}\text{M}_\odot$, where the uncertainty is estimated from a family of lens models that satisfy $\Delta\chi^2\leq 1$. We identify these models by exploring the five–dimensional parameter space defined by the free parameters in the fiducial best–fit model. The observed magnitude of the BCG in the same aperture is $V_{606}(R\leq 2'')=17.5\pm 0.1$. Correcting to the observed V –band and applying both k –correction and galactic extinction (Sand et al. 2003) we obtain $M_V(R\leq 2'')=-22.2\pm 0.2$. The total mass–to–light ratio of A 1201 on the scales probed by the tangential arc projected along the line of sight is therefore $M_{\text{tot}}/L_V=9.4^{+2.4}_{-2.1}(\text{M/L})_\odot$. This number is larger than values typical of stellar populations of early–type galaxies (e.g., Gerhard et al. 2001). Indeed, the joint lensing and dynamical analysis of this cluster by Sand et al. (2003) yields a stellar mass–to–

light ratio of $M_\star/L_V=3.8\pm0.3(M/L)_\odot$. We therefore conclude that 60% of the mass within the cylinder of radius $2''$, i.e. 15% of the effective radius, is in the form of dark matter (i.e. the ratio of stellar to total mass to light ratios).

4. Discussion and Conclusions

4.1. Is A 1201 Unique Among Cluster Lenses?

A 1201 is drawn from a sample of 55 X-ray luminous clusters observed with *HST* in the Edge et al. (PIIDs: 8301 & 8719) snapshot survey of BCGs. This snapshot survey doubles the number of clusters that have been observed to date with either the WFPC2 or ACS cameras. Among these ~ 100 clusters, A 1201 is the only system with a tangential arc on scales as small as $R=2''$. This rarity underlines the importance and efficiency of snapshot surveys with *HST* to discover such small-scale probes of the mass distribution in clusters.

We also investigate the uniqueness of the tangential arc in A 1201 among multiple-image systems in spectroscopically confirmed cluster lenses. The deflection angle of a gravitational lens depends on the angular diameter distance ratio $D_{\text{LS}}/D_{\text{OS}}$ where D_{LS} is the distance from the lens to the source and D_{OS} is the distance from the observer to the source. We plot the distribution of distance ratios for known multiple-image systems in Fig. 2, based on an extensive review of the *HST* archive and the published literature (see Sand et al. 2004, in prep. for more details). The cluster sample upon which this histogram is based is heterogeneous. We therefore also plot (as the dashed histogram) the distribution of distance ratios for the multiple-image systems identified thus far in a well-defined sample of X-ray luminous clusters at $z=0.21\pm0.04$ by Smith (2002; see also Smith et al. 2001, 2002; Kneib et al. 2003, in prep.; Smith et al. 2003, in prep.). A 1201 lies at the lower envelope of both multiple-image samples, with a value of $D_{\text{LS}}/D_{\text{OS}}=0.597$. From a lens geometry perspective, A 1201 is therefore unusual but not unique among the multiple-image systems discovered to date. Other low $D_{\text{LS}}/D_{\text{OS}}$ systems include famous lensing clusters, for example the giant arc ($z=0.724$; Soucail et al. 1988) in A 370 ($z=0.370$). However, the higher redshift of this, and other clusters with low distance ratios renders the observed deflection angle ($\sim 10\text{--}20''$) and the physical scales probed ($\sim 60\text{--}120$ kpc) much larger than that relevant to A 1201 ($R=6$ kpc). A 1201 is therefore unique in the small physical scales probed by its tangential arc.

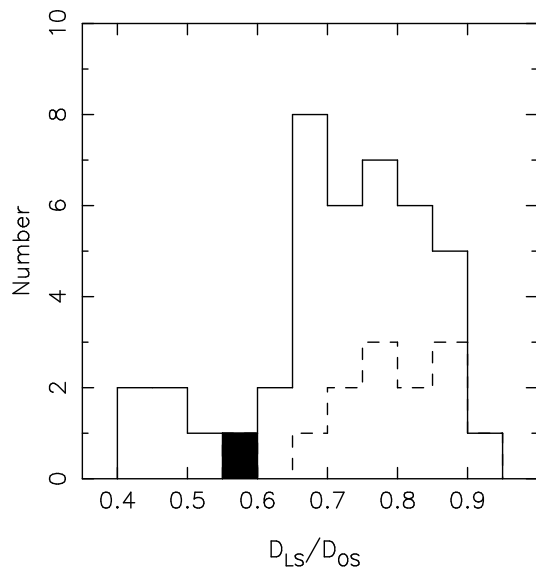


Fig. 2.— The distribution of $D_{\text{ls}}/D_{\text{os}}$ for observed multiple-image systems, drawn from an extensive search of the *HST* archive and the published literature (Sand et al. 2004, in prep.). The solid histogram shows the full sample of 41 multiple-image systems; the dashed histogram shows a sample drawn from a well-defined sample of X-ray luminous clusters (Smith 2002); the filled histogram marks the location of A 1201.

4.2. Summary and Outlook

HST snapshot imaging of A 1201 ($z=0.169$) with the WFPC2 camera reveals a tangential arc 2–arcsec from the center of this cluster. Spectroscopy obtained with ESI on the Keck-II telescope confirms the gravitational nature of the arc, and places the source galaxy at $z=0.451$. We construct a gravitational lens model that is able to reproduce the observed arc morphology. The key feature of this model is that the total matter distribution is significantly more elongated ($\epsilon_{\text{total}} \geq 0.5$) than the light distribution of the BCG on 2'' scales ($\epsilon_{\text{BCG}} = 0.23 \pm 0.03$). With the current data we are unable to determine whether the matter distribution really is more elongated than the stellar distribution, or if there is a significant amount of mass whose center of mass does not coincide with the BCG. This could indicate that the cluster is dynamically less mature than the optical data suggest.

The proximity of the arc to the center of this cluster is unique among cluster lenses, and provides an important constraint on the mass of the cluster on very small physical scales. We measure the projected mass within the tangential arc to be $M(R \leq 2'') = (5.9^{+0.9}_{-0.7}) \times 10^{11} M_{\odot}$, and the V –band mass–to–light ratio to be $M/L(R \leq 2'') = 9.4^{+2.4}_{-2.1} (M/L)_{\odot}$, the angular scale of 2'' corresponding to a physical scale of 6 kpc. This constraint, in conjunction with complementary high–resolution space–based data from *Chandra* and multi–color follow–up with *HST*/ACS will lead to substantial progress in understanding the distribution of mass in this cluster. Extending the unique small–scale (6 kpc) mass constraint out to larger scales (~ 50 –500 kpc) also promises an important role for A 1201 in the quest to understand the physical processes at play in galaxy cluster cores.

Acknowledgments

GPS thanks Jean–Paul Kneib for sharing his LENSTOOL ray–tracing code and Chuck Keeton for discussions about lens statistics. We also thank Richard Ellis for assistance with the Keck observations. We are grateful for financial support from the Royal Society (ACE, SWA) and NASA (DJS, TT) through grant HST–AR–09527. TT acknowledges support from NASA through Hubble Fellowship grant HF-01167.01.

REFERENCES

- Allen S.W., 1998, MNRAS, 296, 392
- Allen S.W., Schmidt R.W., Fabian A.C., 2002, MNRAS, 335, 256

- Arabadjis J.S., Bautz M.W., Garmire G.P., 2002, ApJ, 572, 66
- Cole S., Lacey C.G., Baugh C.M., Frenk C.S., 2000, MNRAS, 319, 204
- Czoske O., Kneib J.-P., Soucail G., Bridges T.J., Mellier Y., Cuillandre J.-C., 2001, A&A, 372, 391
- Ebeling H., et al., 1998, MNRAS, 301, 881
- Kassiola A., Kovner I., 1993, ApJ, 417, 450
- Kneib J.-P., 1993, PhD Thesis, Université Paul Sabatier, Toulouse, France
- Kneib J.-P., Ellis R.S., Smail I., Couch W.J., Sharples R.M., 1996, ApJ, 471, 643
- Kneib J.-P., Hudelot P., Ellis R.S., Treu T., Smith G.P., Marshall P., Czoske O., Smail I., Natarajan P., 2003, ApJ, in press, astro-ph/0307299
- Lewis A.D., Buote D.A., Stocke J.T., 2003, ApJ, 586, 135
- Miralda-Escudé J., 2002, ApJ, 564, 60
- Sand D.J., Treu T., Ellis R.S., 2002, ApJ, 574, L79
- Sand D.J., Treu T., Smith G.P., Ellis R.S., 2003, ApJ, submitted, astro-ph/0309465
- Sheinis A.I., et al., 2002, PASP, 114, 851
- Smith G.P., Kneib J.-P., Ebeling H., Czoske O., Smail I., 2001, ApJ, 552, 493
- Smith G.P., 2002, PhD Thesis, University of Durham, UK, available upon request from gps@astro.caltech.edu
- Smith G.P., Edge A.C., Eke V.R., Nichol R.C., Smail I., Kneib J.-P., 2003, ApJ, 590, L79
- Soucail G., Mellier Y., Fort B., Mathez G., Cailloux M., 1988, A&A, 191, L19
- Spergel D.N., Steinhardt P.J., 2000, Phys. Rev., 84, L3760
- Swinbank A.M., Smith J., Bower R.G., Bunker A., Smail I., Ellis R.S., Smith G.P., Kneib J.-P., Sullivan M., Allington-Smith J.R., 2003, ApJ, in press, astro-ph/0307521